

## Supporting Information

### Regulation of radicals from electrochemical exfoliation of double-graphite electrode to fabricate high-quality graphene

Le Li, Minqiang Wang\*, Jun Guo, Minghui Cao, Hengwei Qiu, Liyan Dai, Zhi Yang

Electronic Materials Research Laboratory, Key Laboratory of the Ministry of

Education & International Center for Dielectric Research, Xi'an Jiaotong University,

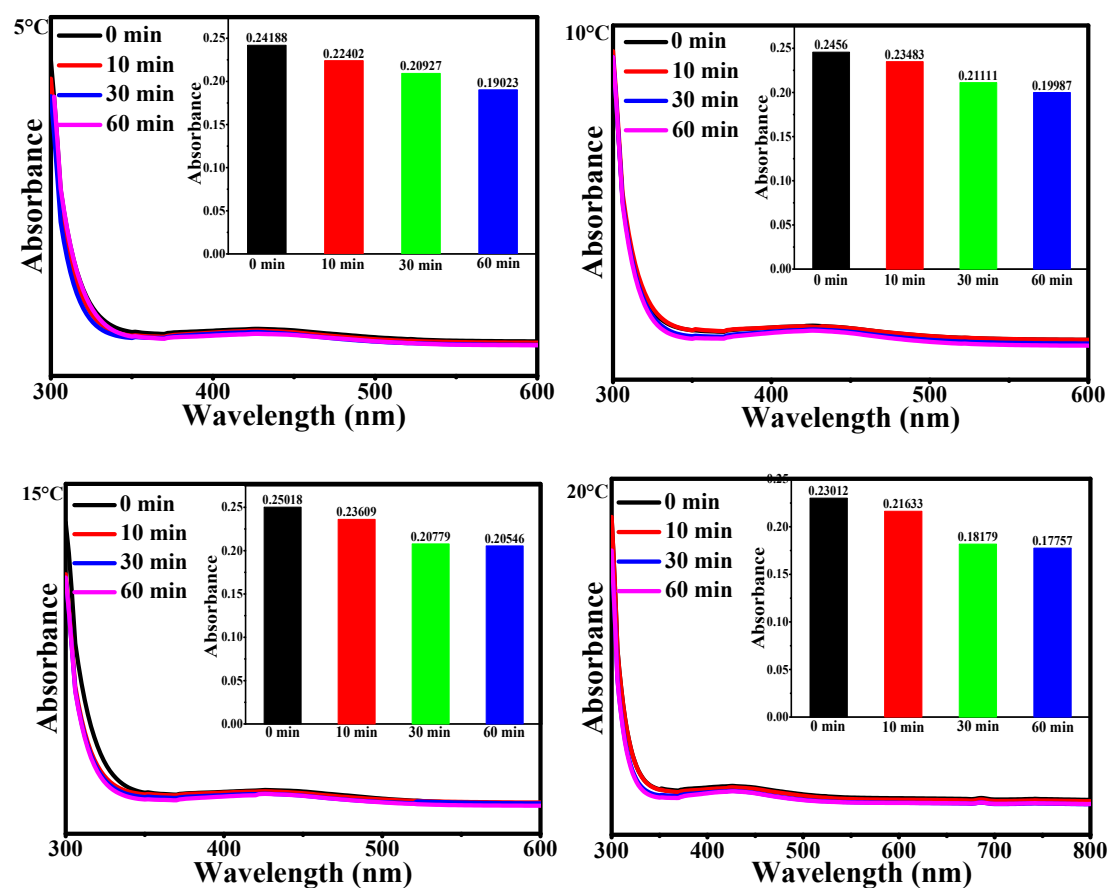
Xi'an 710049, China

Shaanxi Engineering Research Center of Advanced Energy Materials & Devices,

Xi'an Jiaotong University, Xi'an, China

\* Corresponding author: Minqiang Wang

Email: mqwang@xjtu.edu.cn



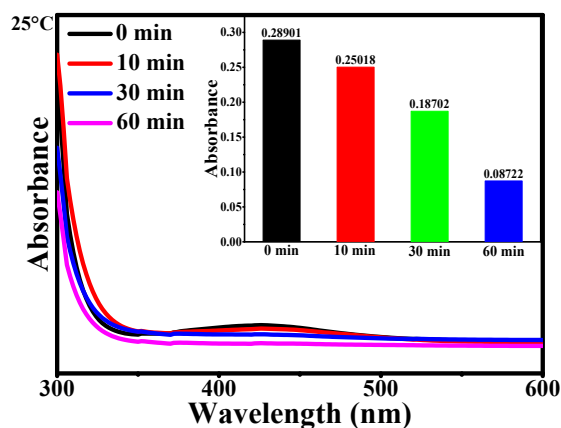


Figure S1 UV-vis spectra of  $1 \text{ mg mL}^{-1}$  TEMPO in  $0.1 \text{ M}$  ammonium sulfate aqueous solution after applying alternating current ( $\pm 10 \text{ V}$ , every 20 seconds from positive ( $+10 \text{ V}$ ) to negative ( $-10 \text{ V}$ )) for 0 min, 10 min, 30 min and 60 min (Graphite foils were used as working electrode and counter electrode).

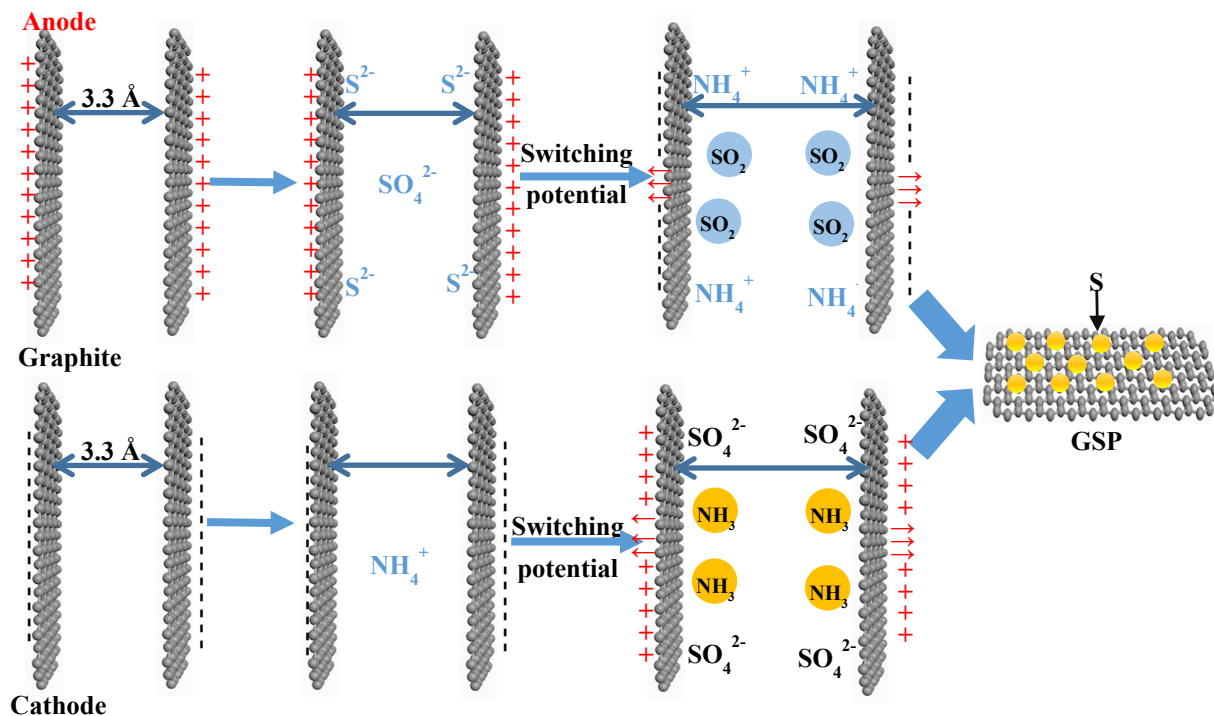
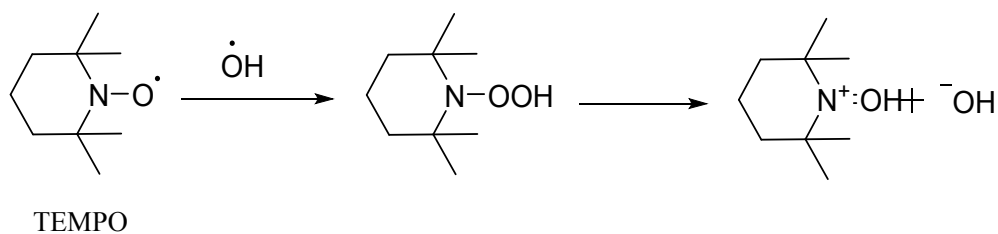


Figure S2. Schematic illustration of the electrochemical exfoliation of double graphite foil and the formation of GSP.

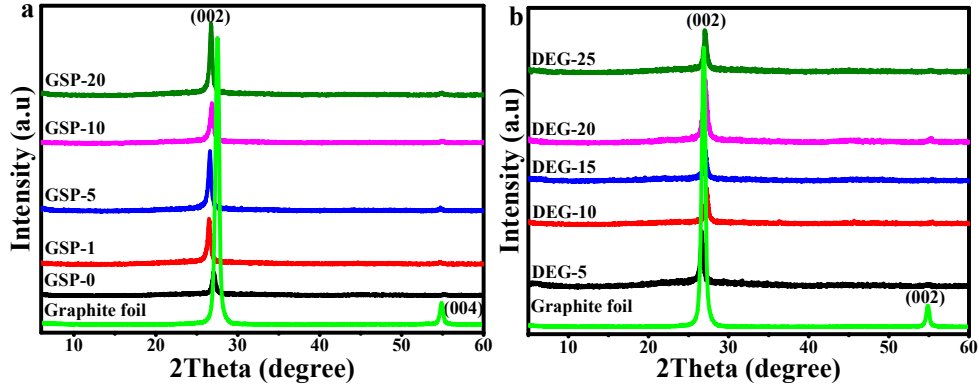


Figure S3. XRD patterns of GSP (a) and DEG (b).

#### Analytical techniques and characterization

The power X-ray diffraction (XRD) analyses were obtained on a XRD-6000 (Japan) spectrometer with Cu Ka ( $\lambda = 0.154$  nm) radiation at 40 kV and 15 mA. The diffraction data was executed in the range of  $2\theta = 5\sim 60^\circ$  with a scan speed of  $10^\circ/\text{min}$ . X-ray photoelectron spectroscopy (XPS) analysis was measured at room temperature on an Thermo Fisher ESCALAB after plasma cleaning for 300 s in the XPS chamber at a pressure of around  $4\times 10^{-8}$  torr. The XPS spectra were peak-differentiated and imitated using the XPS peak 4.1 software in which a shirley background was assumed. The morphological characteristics of graphene were obtained by using SEM Quanta F250 and JEM-2100 transmission electron microscope (Japan Electron Optics Laboratory Co., Ltd., JEOL) with an accelerating voltage of 200 kV.

The samples were measured according to their EMI SE characterization in a frequency range of 8-12 GHz (X-band) using the waveguide method via the vector network analyzer (HP8720ES8720ES). The S parameters ( $S_{11}$  and  $S_{21}$ ) of each sample were recorded and were then used to calculate the EMI SE. The parameter  $S_{11}$  symbolizes the tested reflection coefficient data, and  $S_{21}$  stands for the transmission data. Because of the negative values of the measured  $S_{11}$  and  $S_{21}$ , the values of the  $|S_{11}|$  and  $|S_{21}|$  were identified as the attenuations of reflection and transmission in the incident electromagnetic waves, respectively. The power coefficients of reflection (R), transmission (T), and absorption (A) were evaluated based on the following equations [1-5]:

$$R = |S_{11}|^2, T = |S_{21}|^2,$$

$$A = 1 - R - T \quad (1)$$

Here, the absorption coefficient is given in terms of the power of the incident wave. After the first reflection, the relative intensity of the effective incident wave inside the material is (1-R). Therefore, the coefficient of effective absorbance ( $A_{eff}$ ) can be defined as follows:

$$A_{eff} = (1 - R - T) / (1 - R) \quad (2)$$

The total EMI SE (SET) is also composed of three parts, including reflection (SER), absorption (SEA), and multiple reflections (SEM). The SET can be simplified as follows [1,3]:

$$SE_T = SE_R + SE_A + SE_M \approx SE_R + SE_A \quad (3)$$

Because of its reflectance and effective absorbance, the EMI SE can be described as follows [3-5]:

$$SE_R = -10 \log(1 - R) \quad (4)$$

$$SE_A = -10 \log(1 - A_{eff}) = -10 \log\left(\frac{T}{1 - R}\right) \quad (5)$$

1 Z. Zeng, H. Jin, M. Chen, W Li, L Zhou, Z Zhang, Lightweight and Anisotropic Porous MWCNT/WPU Composites for Ultrahigh Performance Electromagnetic Interference Shielding. *Adv. Funct. Mater.*, 2016, 26, 303.

2 M. H. Al-Saleh, U. Sundararaj, Electromagnetic Interference Shielding Mechanisms of CNT/Polymer Composites, *Carbon*, 2009, 47, 1738.

3 S. Biswas, I Arief, S. S. Panja, S. Bose, Absorption-Dominated Electromagnetic Wave Suppressor Derived from Ferrite-Doped Cross-Linked Graphene Framework and Conducting Carbon. *ACS Appl. Mater. Interfaces*, 2017, 9, 3030.

4 B. Shen, Y Li, D, Yi, W. Zhai, X. Wei, W, Zheng. Strong Flexible Polymer/Graphene Composite Films with 3D Saw-Tooth Folding for Enhanced and Tunable Electromagnetic Shielding. *Carbon*, 2017, 113, 55.

5 X. H. Li, X. Li, K. N. Liao, P. Min, T. Liu, A. Dasari, Z. Z. Yu, Thermally Annealed Anisotropic Graphene Aerogels and Their Electrically Conductive Epoxy Composites with Excellent Electromagnetic Interference Shielding Efficiencies. *ACS Appl. Mater. Interfaces*, 2016, 8, 33230.

6 N Parveen, M. O. Ansari, S. A. Ansaria, M. H. Cho, Simultaneous sulfur doping

and exfoliation of graphene from graphite using an electrochemical method for supercapacitor electrode materials, *J. Mater. Chem. A.*, 2016, 4, 233.